arXiv:1211.6867v1 [quant-ph] 29 Nov 2012

Trapping of Topological-Structural Defects in Coulomb Crystals

M. Mielenz, J. Brox, S. Kahra, G. Leschhorn, M. Albert, and T. Schaetz*
Albert-Ludwigs-Universität Freiburg, Physikalisches Institut,
Hermann-Herder-Strasse 3, 79104 Freiburg, Germany and
Max-Planck-Institut für Quantenoptik, Hans-Kopfermann-Strasse 1, D-85748 Garching, Germany

H. Landa and B. Reznik
School of Physics and Astronomy, Raymond and Beverly Sackler
Faculty of Exact Sciences, Tel-Aviv University, Tel-Aviv 69978, Israel

We study experimentally and theoretically structural defects which are formed during the transition from a laser cooled cloud to a Coulomb crystal, consisting of tens of ions in a linear radiofrequency trap. We demonstrate the creation of predicted topological defects ('kinks') in purely two-dimensional crystals, and also find kinks which show novel dynamical features in a regime of parameters not considered before. The kinks are always observed at the centre of the trap, showing a large nonlinear localized excitation, and the probability of their occurrence surprisingly saturates at ~ 0.5. Simulations reveal a strong anharmonicity of the kink's internal mode of vibration, due to the kink's extension into three dimensions. As a consequence, the periodic Peierls-Nabarro potential experienced by a discrete kink becomes a globally confining potential, capable of trapping one cooled defect at the center of the crystal.

Stable, collective configurations that are non-perturbative, such as solitons, kinks, vortices, monopoles, and other structural defects, have been extensively studied theoretically and experimentally in a variety of fields in physics, ranging from fluid mechanics, condensed matter, atomic physics and optics, to high energy physics and cosmology [1–3]. These nonlinear solutions are localized, particle-like objects that can propagate without dispersing, and acquire stability which can often be explained by their underlying topological nature. Such topological configurations can be formed during a first- or second-order phase transition [4–6], for instance as in the case of vortex defects in a superfluid. Over the last decades, there has been significant interest in the study of topological defects in discrete systems, which can show similar nonlinear phenomena. The Frenkel-Kontorova (FK) model [7], for example, requires a periodic, one-dimensional lattice system, and features much of the effects that are characteristic in its continuum counterpart (sine-Gordon field theory). In discrete systems, solitons are often referred to as kinks, translation-invariance is replaced by lattice-periodicity and the kinks, propagating along the lattice, are subject to the so called Peierls-Nabarro (PN) potential [7]. The experimental study of discrete solitons has been demonstrated in several systems, e.g., in waveguide arrays [8], and proposed with, e. g., cold atoms in optical lattices [9]. Since discrete defects possess substantially less degrees of freedom, they are in many cases experimentally favorable for precise control of their gap-separated, localized modes of oscillation and in particular, for studying quantum coherence effects [10] and quantum information prospects [11, 12].

In particular, cold trapped ions [13] offer a promising platform for studying the formation and structure of topological defects, as well as for the exploration of their quantum properties. When applying laser-cooling to trapped ions, they undergo a transition from a state of a chaotic cloud to an ordered structure, a Coulomb crystal [14]. Isolated from environmental disturbances in ultrahigh vacuum, such crystals forming one-dimensional chains permit investigating quantum effects at the forefront of quantum metrology [15], quantum computing [16, 17] and quantum simulations [18–20]. By adiabatically altering the trapping parameters it is possible to generate phase transitions from the one- (linear) to two- (zigzag) and three-dimensional crystals [21–23]. Such structural transitions have been proposed to permit investigating quantum phase transitions [23, 24].

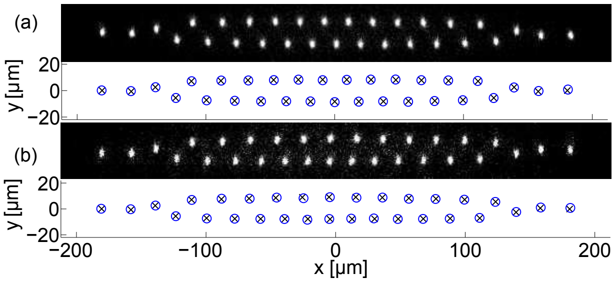

FIG. 1. Coulomb crystals, here with 31 ions ($\omega_z/\omega_y \approx 1.34$). (a) Top: a CCD image of flourescence light of individual ions trapped and laser cooled in a zigzag configuration. Bottom: circles indicate the fitted positions, while crosses depict the expected positions at the given trapping parameters, derived by MD simulations, the deviation remaining within the experimental resolution (see text). (b) As in (a), however, the ions in the center region forming an extended 'kink' defect. While the ions to the left of the center form a zigzag structure as in (a), the positions on the right are mirrored about the x-axis. Such a kink, linking two configurations of an odd number of ions in a circular trap, would be topologically protected.

The experimental creation of localized defects in ion crystals has been achieved during a crystallization of the ion cloud [13]. It has been also suggested that a non-adiabatic change of the trapping potential could trigger the creation of defects during the phase-transition from one- to two-dimensional crystals [25, 26]. Realizations of the FK model with ion strings have been suggested in [27–29]. The quantum mechanical properties of kinks in ion traps have been theoretically explored in [25], and the connection with the inhomogenous Kibble-Zurek mechanism in [26, 30]. Currently the latter is under investigation in several groups, e. g. [31], having created kinks by quenching the radial confinement of the trap.

In this Letter we present the experimental realization of predicted, extended 2D-defects as well as a new class of quasi-3D defects, both induced by laser cooling [32] and long lived in the Doppler-cooling regime. In the thermodynamic limit, as well as in circular configurations [25, 33], similar discrete solitons (kinks) become topologically protected. With respect to these we regard the observed configurations as ‘topological’ defects. For the 3D-kink we directly observe a highly nonlinear oscillation at its localized, gapped mode and reveal that the probability to observe a kink at equilibrium shows an intriguing saturation at ~ 0.5. We study numerically the structural and dynamical properties of these kinks and find that their extention into 3D causes a modification of the Peierls-Nabarro potential, featuring an inherent trapping of the kink at the centre of the Coulomb crystal, and resulting in the observed saturation in the kink’s occurrence.

The experimental setup consists of a linear Paul trap ($\Omega_{\mathrm{rf}} = 2\pi \cdot 6.22\,\mathrm{MHz}$) [34, 35] trapping Coulomb crystals of different size of choice (here 10 - 65 photoionized $^{24}\mathrm{Mg}^{+}$ions). Experiments were carried out at a single ion trapping frequency of $\omega_{\mathrm{x}} \approx 2\pi \cdot 56\,\mathrm{kHz}$ (axial direction), while the radial frequencies were varied in the range of $\omega_{\mathrm{y}} \approx 2\pi \cdot 320\,\mathrm{kHz}$ to $2\pi \cdot 630\,\mathrm{kHz}$, corresponding to a total depth of the rf-trapping potential energy of the order of $\mathrm{k_B}\,10^4\,\mathrm{K}$, $\mathrm{k_B}$ being the Boltzmannfactor. The radial indegeneracy $\omega_{\mathrm{z}}/\omega_{\mathrm{y}}$ is tuned between 1 and 1.4. The ions are Doppler cooled via one laser beam, slightly tilted ($\sim 5°$) with respect to x-axis. It drives the $\mathrm{S}_{1/2}$-$\mathrm{P}_{3/2}$ transition ($\lambda = 280\,\mathrm{nm}$, natural linewidth $\Gamma \approx 2\pi \cdot 42\,\mathrm{MHz}$) and is detuned by $\Delta \approx 2 \cdot \Gamma/2$ at a saturation of about 0.2 (Doppler cooling limit $\mathrm{T_D} \approx 1\,\mathrm{mK}$ at $\Delta = \Gamma/2$). Data is acquired with a CCD-camera detecting fluorescence light of $^{24}\mathrm{Mg}^{+}$to determine the ion positions (see figure 1). The resolution is given by the magnified (10 x) pixelsize ($0.8\,\mu$m) of the image on the CCD-camera. Individual images are integrated for 200 ms. By increasing the axial confinement (decreasing the radial) we reproduce increasingly complex structures, from a linear chain to 3D crystals. At constant confinement, the structure and its dimensionality depend on the number of trapped ions, due to the impact of their space charge density on the total potential.

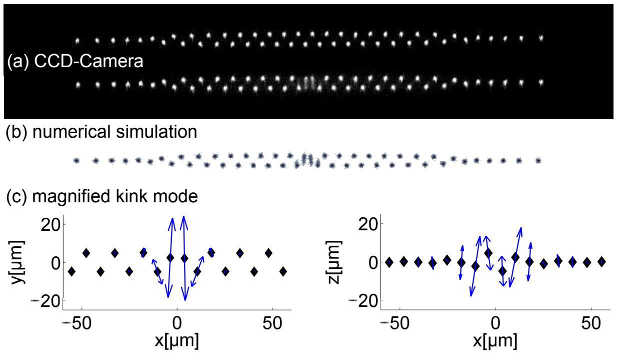

FIG. 2. Coulomb Crystals containing 50 ions, similar to those depicted in figure 1, however for reduced asymmetry of the radial confinement, $\omega_{\mathrm{z}}/\omega_{\mathrm{y}} \approx 1.05$. (a) CCD images of two crystals obtained for identical experimental parameters. Top: a pure zigzag featuring the minimal energy configuration. Bottom: two central ions clearly deviate and show a blurred extension in the radial direction. As in figure 1b, the right parts of the crystals are close to identical while the left part of the lower crystal depicts a flipped ‘zagzig’ structure, separated by the two central ions. (b) Integrated numerical results for the structure depicted in (a)-Bottom, projected onto the crystal plane. The agreement of theory and experiment remains comparable to figure 1. (c) Numersically derived components of ion oscillations in the localized, low-frequency normal mode of the kink (see figure 4b) in (perpendicular to) the crystal plane are depicted on the left (right).

To calibrate our system and to gain a deeper understanding of the structure and the dynamics within the crystals, we numerically simulate our experimental results by a Molecular Dynamics (MD) code [36]. We take into account the full time-dependent trapping potential, and run an optimization routine which considers all trapping parameters and the projection of the crystal plane (xy) on the CCD-chip chosen roughly perpendicular to the z-axis. We reproduce all observed crystals consistently, with a maximal average deviation of 0.5μm per ion, which is less than the pixel size. We obtain identical results in a simulation using a constant harmonic potential, verifying that micromotion [37] does not alter our findings.

In the investigated regime of trapping parameters, for a number of ions between 20 and 60, zigzag structures with and without local defects occur (see figure 1). The duration after which a zigzag-structure gets destroyed, for example, by a collision with constituents of the background gas, amounts to 10 seconds. The lifetime of structural defects within crystals amounts to the same order of magnitude and exceeds the natural timescale for oscillations of the normal modes in the Coulomb crystals ($\sim 1/\omega_{\mathrm{x}}$) by five orders of magnitude. The two different structures imaged by the CCD-camera, depicted in figure 1, are obtained for $\omega_{\mathrm{z}}/\omega_{\mathrm{y}} \approx 1.34$, where ω_{z} is the in-plane and ω_{y} is the out-of-plane radial trapping fre-

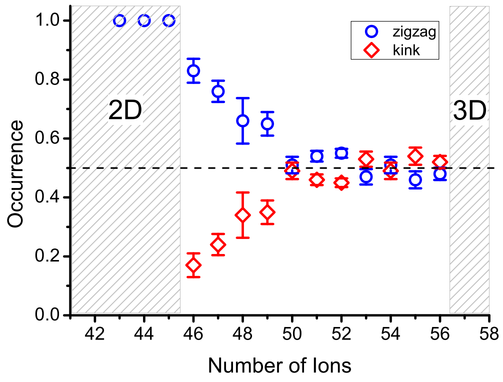

FIG. 3. Probability for the occurence of a pure zigzag and a zigzag with a kink as depicted in figure 2, formed during a nonadiabatic, cooling-induced transition from a cloud to a crystal, for identical trapping parameters, plotted in dependence of the number of ions. With 27 ions and more the minimum energy configuration at our set of trapping parameters is a zigzag structure (blue circles). Starting with 46 ions, we observe an increasing probability for a zigzag structure with one kink (red rhomb) at the centre of the crystal. No simultaneous occurrence of two or more defects is observed. Surprisingly, the probability for observing one kink saturates at ~ 0.5 (dashed line) for up to 56 ions (see explanation in the text). Error bars represent the statistical error ($1\,\sigma$).

quency. Whereas figure 1a presents the established zigzag configuration, which is the global minimum of potential energy, figure 1b depicts a local minimum, incorporating an extended kink, as predicted in [25]. The zigzag structures considered so far are extended in two dimensions (xy) only, independent of the presence of a kink. Keeping the axial confinement constant and lowering ω_z/ω_y, we create qualitatively new defects (figure 2a). For the rest of this paper we discuss their occurrence and properties on the exemplary set of parameters of $\omega_z/\omega_y \approx 1.05$. In this regime, zigzag structures without a kink occur starting with 27 ions and remain two-dimensional with up to 52 ions. With 53 ions, a structural phase transition into 3D can be deduced from the numerical results, the space charge of the ions defocussing a few central ions slightly out of the zigzag plane (by $\lesssim 1\,\mu$m). Further increasing the number of ions causes a growing fraction of the ions to extend into the z-direction, however, the global minimum configuration (which remains close to a planar zigzag) is still unambigously identifiable. For more than 56 ions no zigzag structures are observed anymore, and we observe projections of complex, helical structures.

Starting with 46 ions, we detect the random occurrence of local defects mainly involving two ions. The directly observable features of the novel class of kinks are: (i) They sustain a large motional amplitude of the two ions along the y-axis, comparable to the radial extension of the crystal, causing the blurring of their images (see figure 2a). (ii) The probability for the occurrence of a kink increases with increasing the number of ions, and saturates at $\sim$ 0.5 for more than 50 ions (see figure 3). (iii) Kinks occur at the center of the crystal only. In order to elucidate feature (i), we use MD simulations as described above and reproduce the positions of the ions and their dynamics in the xy-plane (see figure 2b). The crystals including one defect remain nearly identical to a pure zigzag, except at the center. There, despite the stiffer $\omega_z > \omega_y$ confinement, the central ions extend into the transverse (z) direction (see figure 2c), even for parameters such that the zigzag crystal without a defect is still planar. We further investigate the properties of the kinks numerically applying two separate approaches: (1) a linearization of the oscillations of the ions at small amplitudes; (2) simulating the adiabatic dynamics of the kinks as they move along the lattice.

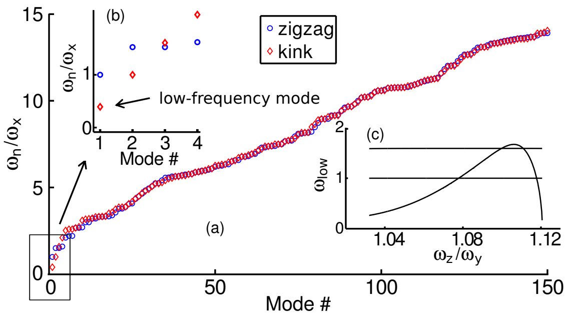

FIG. 4. Dispersion relations for a crystal of 50 ions as in figure 2, with (red rhombs) and without (blue circles) a kink. (a) The spectra of normalized frequencies ω_n/ω_x of the 150 normal modes remain close to identical for the most part. (b) A magnified inset showing that the kink configuration has a low-frequency mode separated by a gap. It is localized to the central ions only, and causes their blurring in the xy-plane (see figure 2a). (c) The normalized frequency of the localized low-frequency mode ω_{low} for a given number of ions, can be controlled by tuning the ratio ω_z/ω_y (here reaching up to $\omega_{\mathrm{low}} \sim 2\,\omega_x$). When the frequency of the lowest mode approaches zero, the configuration including the kink undergoes a structural phase transition.

The dispersion relations for the pure zigzag and the crystal with the centered kink (figure 2) are shown in figure 4. For the largest fraction, both structures exhibit indistinguishable mode spectra. However, whereas the lowest mode of the zigzag is the axial center of mass mode (with the frequency ω_x), the kink features a gapped mode below ω_x (see figure 4a, b), localized on the center ions. A dynamical simulation assuming a thermal energy of $k_B T_D$ for all modes and integrating a 'fluorescence' image from the numerically obtained ion trajectories, reproduces accurately the blurring of the central ions (see figure 2b). We numerically confirm that this effect is not caused by micromotion or by the near-axial incidence of the cooling laser, and that it remains unaffected assuming a realistic equilibrium temperature of $\sim 5\,\mathrm{T_D}$. In fact, the apparent blurring of the center ions is reproduced exactly, even assuming an excitation of the low-frequency mode only. A careful analysis of the dynamics [36] reveals that the large-amplitude motion is due to the highly anharmonic oscillation of the ions on the localized low-frequency mode of the kink. In addition, the frequency of the low energy mode, ω_{low}, can be controlled by tuning the radial trapping frequencies $\omega_{\mathrm{z}}/\omega_{\mathrm{y}}$ over a range of 0 to $\sim 2\,\omega_{\mathrm{x}}$ (see figure 4c).

To further elucidate features (ii) and (iii) of the observed kinks, we focus on this mode that describes the ion oscillations near a minimum of the Peierls-Nabarro (PN) potential. For ion crystals of constant ion density, e. g. in a circular trap [25, 33] or in an anharmonic trap [38], the PN potential is periodic with the inter-ion distance. For a zigzag in a harmonic trap, the space charge density and the radial displacement decrease out of the centre of the crystal. If $\omega_{\mathrm{z}}/\omega_{\mathrm{y}} \gg 1$, the depth of the local minima of the PN potential decreases progressively towards the sides [26, 30], where the kink can dissolve into the linear chain at each of the ends, after a random walk [39].

To analyze the motion of the 3D-defect along the lattice for our case of $\omega_{\mathrm{z}}/\omega_{\mathrm{y}} \gtrsim 1$, we run a dynamical MD simulation for a kink created initially at an off-centered position. We follow its adiabatic dynamics while cooling the motional degrees of freedom of the ions to overdamp the dynamics. We find that the kink ‘slides’ down towards the center of the crystal within an effective trapping potential. Tracing the ‘downhill’ motion of the kink allows to calculate the potential along the adiabatic kink trajectory. We reveal that the effective PN potential is no longer periodic, but rather modified to an overall harmonic potential of a global depth quadratically depending on the total number of ions (see figure 5b). Similarly, since the planar extended kink of figure 1 expands more at its centre than the zigzag configuration, the PN potential is modified in the crystal plane such that this kink is stable only at the centre.

For 44 ions, we derive from the simulation the global potential depth for a kink within the crystal to be roughly $10\,\mathrm{k_B T_D}$ (figure 5a). This is the height of the barrier for the kink’s escape to the sides where it is lost, and the relevant degree of freedom for the propagation of the kink is its localized mode. The minimal equilibrium temperature of the ions in the experiment can be estimated to amount to a few times $\mathrm{T_D}$. Therefore, during crystallization and formation of the defects, a kink can be created with sufficient energy to escape its trapping potential. However, the potential depth for a kink rises with the number of ions such that for 46 ions, it already amounts to $\sim\!20\,\mathrm{k_B T_D}$, permitting to trap the defect with higher probability within the Coulomb crystal. Since the minimum configuration has a $\mathbb{Z}_2$ symmetry (of a zigzag and its mirror-image), the defect following a kink must be its anti-kink. All defects created within the trapping region will slide to the center and pairwise annihilate, either leaving one centered kink (if the initial number of kinks was odd), or none. Although we are not yet capable to observe this process directly, these considerations provide a consistent explanation for the experimental occurrence of one centred kink remaining at ~ 0.5 for the whole range of 50-56 ions (see figure 3), with the small noticeable oscillation possibly indicative of the underlying dynamics. Additionally, it will be interesting to analyze the interplay of thermal effects with the increase in the number of kinks being formed during the crystallization as the number of ions is increased.

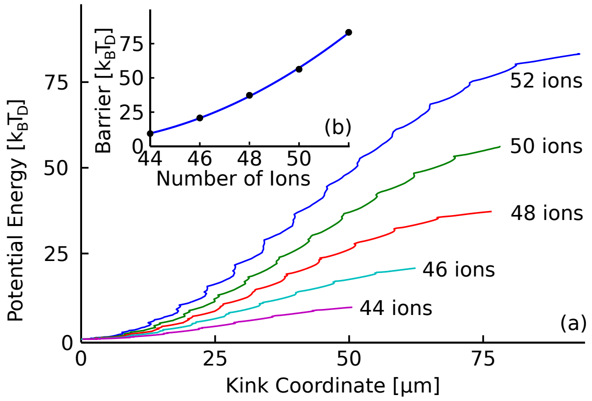

FIG. 5. Simulation of the effective PN potential energy of a kink (see figure 2), (a) dependent on its distance from the center of the Coulomb crystal. The potential is symmetric about the trap center, and reaches its maximum roughly at the final values shown (dependent on the total ion number). Beyond the related displacements, the kink will ‘slide’ to the side and dissolve. (b) The total potential barrier for the kink to escape its trap by reaching the sides is given in dependence of the number of ions, fitted by a quadratic function (blue line).

Entering the quantum regime for large Coulomb crystals and 2D structures by exploiting the kinks’ localized properties is another interesting step. Cooling the localized gapped mode to the motional ground state and studying its coupling to the bath consisting of the rest of the modes would permit to explore mesoscopic open quantum systems. The controllable trapping parameters offer the possibility to shape the characteristics of the kinks, e. g. by tuning the frequency and gap of the localized mode as described above. The ‘kink trap’ storing kinks at the center of the Coulomb crystal will be exploited for studying the interaction of different classes of defects (such as a kink combined with a mass defect or a second kink protected by a mass-defect, that we have observed and will describe elsewhere [36]). These cannot annihilate, but yet are forced into a short range interaction in a quasi-deterministic way.

TS was funded by the Deutsche Forschungsgemeinschaft (SCHA973), TS and BR acknowledge the support of the European Commission (STREP PICC). BR acknowledges the support of the Israel Science Foundation and the German-Israeli Foundation.

---

* tobias.schaetz@physik.uni-freiburg.de

[1] N. D. Mermin, Rev. Mod. Phys. **51**, 591 (1979).

[2] R. Rajaraman, *Solitons and Instantons*, North-Holland Personal Library (North-Holland, 1987).

[3] T. Dauxois and M. Peyrard, *Physics of Solitons* (Cambridge University Press, 2006).

[4] T. W. B. Kibble, Journal of Physics A **9**, 1387 (1976).

[5] T. Kibble, Physics Reports **67**, 183 (1980).

[6] W. H. Zurek, Nature (London) **317**, 505 (1985).

[7] O. Braun and Y. Kivshar, *The Frenkel-Kontorova Model*, Texts and Monographs in Physics (Springer, 2004).

[8] F. Lederer, S. Darmanyan, and A. Kobyakov, Springer Series in Optical Sciences **82**, 269 (2001).

[9] A. Trombettoni and A. Smerzi, Phys. Rev. Lett. **86**, 2353 (2001).

[10] A. Wallraff, A. Lukashenko, J. Lisenfeld, A. Kemp, M. Fistul, Y. Koval, and A. Ustinov, Nature **425**, 155 (2003).

[11] T. Fujii, M. Nishida, and N. Hatakenaka, Phys. Rev. B **77**, 024505 (2008).

[12] S. Marcovitch and B. Reznik, Phys. Rev. A **78**, 052303 (2008).

[13] C. Schneider, D. Porras, and T. Schaetz, Reports on Progress in Physics **75**, 024401 (2012).

[14] R. Blumel, J. M. Chen, E. Peik, W. Quint, W. Schleich, Y. R. Shen, and H. Walther, Nature **334**, 309 (1988).

[15] C. W. Chou, D. B. Hume, J. C. J. Koelemeij, D. J. Wineland, and T. Rosenband, Phys. Rev. Lett. **104**, 070802 (2010).

[16] P. Schindler, J. T. Barreiro, T. Monz, V. Nebendahl, D. Nigg, M. Chwalla, M. Hennrich, and R. Blatt, Science **332**, 1059 (2011).

[17] J. P. Home, D. Hanneke, J. D. Jost, J. M. Amini, D. Leibfried, and D. J. Wineland, Science **325**, 1227 (2009).

[18] J. I. Cirac and P. Zoller, Nat Phys **8** (2012), 10.1038/nphys2275.

[19] D. Porras and J. I. Cirac, Phys. Rev. Lett. **92** (2004).

[20] C. Wunderlich, *Laser Physics at the Limit* (Springer, Heidelberg, 2002) pp. 261–273.

[21] J. P. Schiffer, Phys. Rev. Lett. **70**, 818 (1993).

[22] G. Piacente, I. V. Schweigert, J. J. Betouras, and F. M. Peeters, Phys. Rev. B **69**, 045324 (2004).

[23] S. Fishman, G. De Chiara, T. Calarco, and G. Morigi, Physical Review B **77**, 064111 (2008).

[24] J. D. Baltrusch, C. Cormick, and G. Morigi, Phys. Rev. A **86**, 032104 (2012), arXiv:1206.4171 [quant-ph].

[25] H. Landa, S. Marcovitch, A. Retzker, M. B. Plenio, and B. Reznik, Phys. Rev. Lett. **104**, 043004 (2010).

[26] A. del Campo, G. De Chiara, G. Morigi, M. B. Plenio, and A. Retzker, Phys. Rev. Lett. **105**, 075701 (2010).

[27] I. García-Mata, O. V. Zhirov, and D. L. Shepelyansky, European Physical Journal D **41**, 325 (2007), arXiv:cond-mat/0606135.

[28] T. Pruttivarasin, M. Ramm, I. Talukdar, A. Kreuter, and H. Häffner, New Journal of Physics **13**, 075012 (2011), arXiv:1104.0451 [quant-ph].

[29] C. Cormick and G. Morigi, Physical Review Letters **109**, 053003 (2012), arXiv:1203.0470 [quant-ph].

[30] G. D. Chiara, A. del Campo, G. Morigi, M. B. Plenio, and A. Retzker, New Journal of Physics **12**, 115003 (2010).

[31] Priv. comm. T. E. Mehlstäubler.

[32] The initially hot ion cloud, including the cooling laser and the ion trap, is an open system and the crystallization is a complex non-adiabatic process, interesting and currently not sufficiently understood by itself.

[33] T. Schätz, U. Schramm, and D. Habs, Nature **412** (2001).

[34] S. Kahra, G. Leschhorn, M. Kowalewski, A. Schiffrin, E. Bothschafter, W. Fusz, R. de Vivie-Riedle, R. Ernstorfer, F. Krausz, R. Kienberger, and T. Schaetz, Nat Phys **8**, 238 (2012).

[35] G. Leschhorn, S. Kahra, and T. Schaetz, Applied Physics B: Lasers and Optics **108**, 237 (2012).

[36] H. Landa, B. Reznik, M. Mielenz, J. Brox, S. Kahra, G. Leschhorn, M. Albert, and T. Schaetz, in preparation.

[37] H. Landa, M. Drewsen, B. Reznik, and A. Retzker, New Journal of Physics **14**, 093023 (2012).

[38] G.-D. Lin, S.-L. Zhu, R. Islam, K. Kim, M.-S. Chang, S. Korenblit, C. Monroe, and L.-M. Duan, EPL (Europhysics Letters) **86**, 60004 (2009).

[39] The shape of the PN potential can be obtained numerically, following adiabatically the trajectory of the kink along the lattice [7]. Starting with an axially displaced kink at rest, at the bottom of its local PN potential well, the localized kink mode vector defines the direction for the motion of the kink to the next lattice site. However, along this trajectory, a localized discrete kink is far from equilibrium, and the macroscopic change of the configuration results in a significant modification of the potential energy landscape. In addition, the modes of the expansion about the minimum become strongly coupled and the moving kink radiates its kinetic energy into all of the lattice modes. Therefore, deriving the PN potential becomes highly nontrivial for discrete kinks.